

Magnetic excitations in charge-ordered $\text{Nd}_{0.5}\text{Ca}_{0.5}\text{MnO}_3$: A Brillouin scattering study

P. MURUGAVEL^{1,2}, C. NARAYANA¹, A. K. SOOD^{1,2}, S. PARASHAR¹,
A. R. RAJU¹ and C. N. R. RAO^{1,2}

¹ *Chemistry and Physics of Materials Unit, Jawaharlal Nehru Centre for Advanced Scientific Research - Jakkur P.O., Bangalore 560 064, India*

² *Indian Institute of Science - Bangalore 560 012, India*

(received 20 June 2000; accepted in final form 18 September 2000)

PACS. 78.35.+c – Brillouin and Rayleigh scattering; other light scattering.

PACS. 75.30.Ds – Spin waves.

PACS. 75.50.-y – Studies of specific magnetic materials.

Abstract. – Brillouin scattering studies on single crystals of a charge-ordered manganite, $\text{Nd}_{0.5}\text{Ca}_{0.5}\text{MnO}_3$, have been carried out for the first time. The spectra show two modes at ~ 27 GHz (B-mode) and 60 GHz (S-mode). The B-mode frequency and intensity from 300 K to 27 K, covering both the charge ordering transition at 250 K and the antiferromagnetic transition, at 170 K, exactly follow the same temperature dependence as the d.c. magnetic susceptibility. The B-mode is associated with bulk magnetic excitations and the S-mode with surface magnetic excitations of the manganite with ferromagnetic correlations. The study is strongly indicative of the presence of ferromagnetic inhomogeneities in the charge-ordered as well as antiferromagnetic phases.

The ground state of doped manganites, with general formula $\text{R}_{1-x}\text{A}_x\text{MnO}_3$ (R = rare-earth, *e.g.* La, Pr, A = alkaline earth metal, *e.g.* Ca, Sr), can be a ferromagnetic (FM) metal or a charge-ordered insulator, depending on the amount of doping x and the tolerance factor [1, 2]. When the weighted average of A site cation radius is small, the Mn-O-Mn bond angle deviates from 180° , reducing the transfer integral and hence the e_g electron bandwidth of Mn^{3+} ions. This causes real space ordering (charge ordering) of the Mn^{3+} and Mn^{4+} ions. Ferromagnetism in the manganites is qualitatively understood in terms of Zener's double exchange which connects electron hopping with the FM alignment of the Mn t_{2g} electron spins [3]. In recent years, charge localisation has been invoked along with double exchange due to the lattice polarons formed by Jahn-Teller (JT) distortion around the Mn^{3+} ions [4]. The formation of magnetic polarons to localise the charge carriers has also been proposed [5].

Recent electron and neutron diffraction experiments have shown the coexistence of an incommensurate charge-ordered phase within the FM metallic phase in $\text{La}_{0.5}\text{Ca}_{0.5}\text{MnO}_3$ [6]. The incommensurate state is considered to involve partial orbital ordering in spite of complete

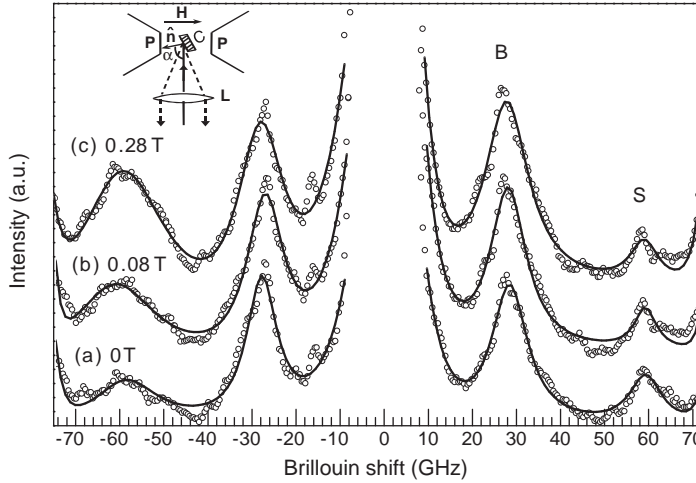


Fig. 1 – Brillouin spectra at different external magnetic field, (a) $H = 0$ T, (b) 0.08 T and (c) 0.28 T. The inset shows the scattering geometry where the magnetic field H (nearly perpendicular to the plane of the sample C) is generated by the electromagnet P. α is the angle of incidence with respect to the normal \hat{n} . The scattered light is collected using the lens L. Open circles are data points and solid lines are fits to Lorentzian functions with appropriate background.

charge ordering. A transmission electron microscopy study of insulating $\text{Pr}_{0.5}\text{Ca}_{0.5}\text{MnO}_3$ has shown the occurrence of the incommensurate-to-commensurate charge ordering transition coincident with the antiferromagnetic (AFM) spin ordering transition at 180 K [7]. We have carried out the first Brillouin scattering study of a charge-ordered manganite to examine magnetic excitations across the charge ordering and AFM transitions to elucidate the role of couplings between the lattice, the charge carriers and the magnetic excitations. For this purpose, we have chosen $\text{Nd}_{0.5}\text{Ca}_{0.5}\text{MnO}_3$ which, like $\text{Pr}_{0.5}\text{Ca}_{0.5}\text{MnO}_3$, remains an insulator at all temperatures and shows a transition from a paramagnetic (PM) insulating state to a charge-ordered (CO) state ($T_{\text{CO}} = 250$ K) and from the CO state to an AFM state ($T_{\text{N}} = 150$ K) [8].

Polycrystalline $\text{Nd}_{0.5}\text{Ca}_{0.5}\text{MnO}_3$ was prepared by the solid-state reaction of Nd_2O_3 , CaCO_3 and MnO_2 at 1273 K for 24 h, followed by sintering at 1373 K for 24 h in flowing oxygen. Powder X-ray diffraction at room temperature showed the material to be orthorhombic with a Mn^{4+} content $\sim 52\%$ as determined by redox titration [8]. The single crystals of $\text{Nd}_{0.5}\text{Ca}_{0.5}\text{MnO}_3$ were grown using floating zone furnace (NEC, Japan). The T_{CO} and T_{N} were measured from the magnetisation measurements using the vibrating sample magnetometer (VSM) (Model No. 7300, LakeShore, USA).

Brillouin scattering measurements were carried out on a disk of 6 mm diameter and thickness of ~ 3 mm cut from the single crystalline rod of $\text{Nd}_{0.5}\text{Ca}_{0.5}\text{MnO}_3$. Spectra were excited using single-mode 532 nm radiation from diode-pumped frequency-doubled Nd-YAG laser (Coherent Model DPSS No. 532-400) in the backscattering geometry with angle of incidence of $\alpha = 65^\circ$ and polarisation in the plane of the incidence. Spectra were recorded using (3+3) pass tandem Fabry-Perot interferometer (JRS Scientific Instruments, Switzerland) with a finesse of ~ 100 and free spectral range of 85 GHz [9]. The temperature-dependent measurements were carried out from 300 K to 27 K with the crystal inside a closed-cycle helium cryostat, with the temperature stability of ± 0.01 K. Measurements were also carried out at room temperature

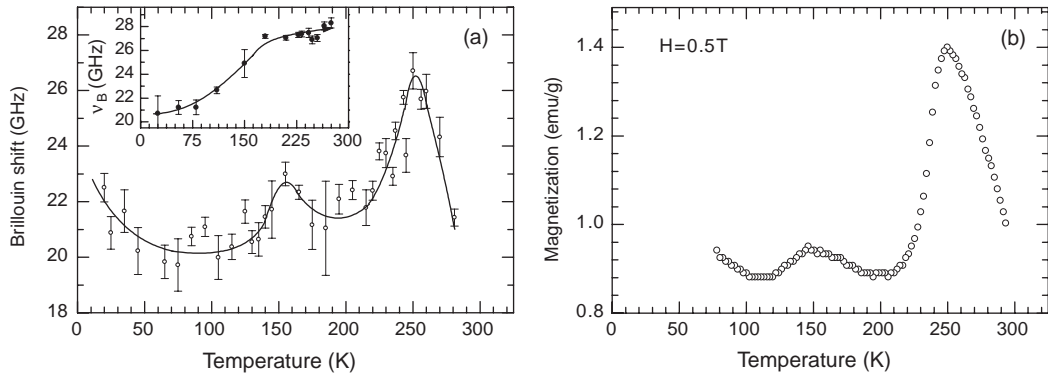


Fig. 2 – (a) Temperature dependence of the B-mode in the cooling cycle. The inset in (a) shows the temperature dependence of the B-mode in the heating cycle. (b) Temperature dependence of magnetisation measured using VSM in a field of 0.5 T. The solid lines are drawn as a guide to the eye.

in the presence of magnetic field (up to 0.3 T using an electromagnet), nearly perpendicular to the plane of the sample, as shown in the inset of fig. 1.

Figure 1 (curve (a)) shows a typical Brillouin spectrum of $\text{Nd}_{0.5}\text{Ca}_{0.5}\text{MnO}_3$ at room temperature in the absence of a magnetic field. Here the data are shown by open circles and the solid lines are fits to Lorentzian with appropriate background. The inset shows the scattering geometry. Two modes at frequencies $\nu_B \sim 27$ GHz (labelled B mode) and $\nu_S \sim 60$ GHz (labelled S mode) are easily identified in the spectra. The S-mode is weak at room temperature and remains so even at lower temperatures. We have therefore followed only the B-mode as a function of temperature. Figure 2(a) shows the temperature dependence of the B-mode frequency (ν_B) and fig. 3, the temperature dependence of its intensity (A) and full-width at half-maximum (Γ) from 300 K to 27 K in the cooling run. Interestingly, ν_B and A closely follow the temperature dependence of the d.c. magnetic susceptibility of the

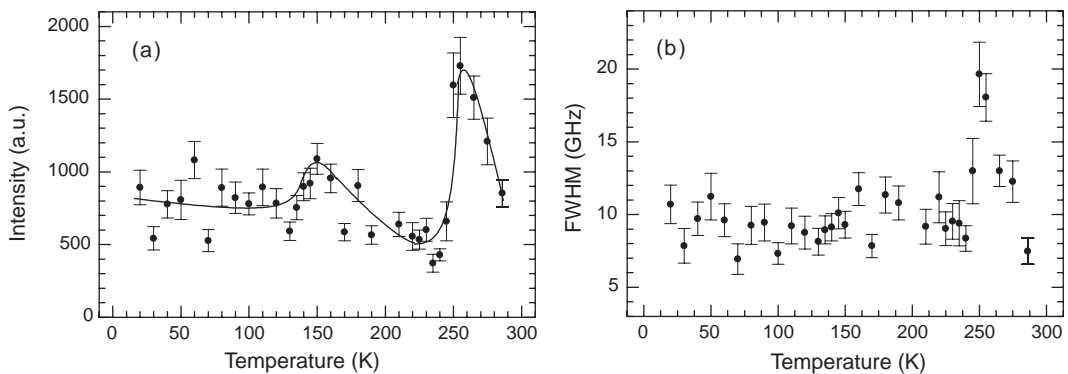


Fig. 3 – Temperature dependence of (a) intensity and (b) linewidth of the B-mode. The solid line is drawn as a guide to the eye.

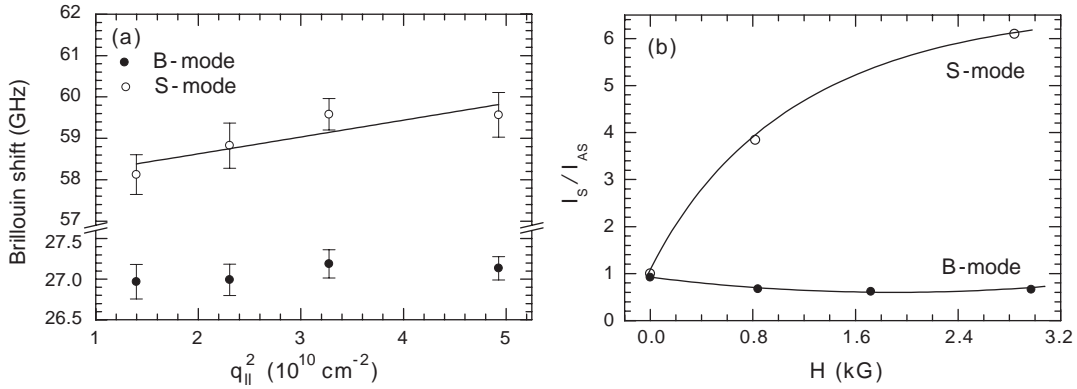


Fig. 4 – (a) Mode frequencies as a function of q_{\parallel}^2 . The solid line is a fit to the linear equation. (b) Ratio of Stokes and anti-Stokes intensities as a function of applied magnetic field at room temperature. The solid lines are a guide to the eye.

same sample shown in fig. 2(b). The observation that ν_B and A are both proportional to the d.c. magnetic susceptibility (χ) strongly suggests that the B-mode is associated with the magnetic excitations of the medium. To check this further, experiments were carried out at room temperature as a function of total wave vector transfer q and its component parallel to the surface, q_{\parallel} . The dependence on q is not entirely conclusive due to the limited range of available q (4 to $4.5 \times 10^5 \text{ cm}^{-1}$). However, the S-mode frequency varies as a function of q_{\parallel} as shown in fig. 4(a). These experiments were done in the backscattering geometry with varying angle α which keeps q constant. It is seen that the B-mode does not depend on q_{\parallel} whereas the S-mode frequency increases linearly with q_{\parallel}^2 , suggesting thereby that the S-mode is associated with surface magnon excitations and the B-mode with bulk magnons. This is further corroborated by the hysteresis observed in the temperature dependence of ν_B as shown in the inset of fig. 2(a) because such hysteresis is not normally expected to occur for acoustic phonons.

It is known that the intensity and peak position of Brillouin lines originating from magnons depend on the external applied magnetic field. Experiments were, therefore, carried out at room temperature with the sample in a magnetic field up to 0.28 T. Curves (b) and (c) in fig. 1 correspond to the spectra at 0.08 and 0.28 T, respectively. The peak positions do not change (to be discussed later), whereas the ratio of the Stokes to anti-Stokes intensities changes significantly for the S-mode, as shown in fig. 4(b). This change can occur because of the non-reciprocal propagation of the Damon-Eshback (DE) surface magnon mode [9, 10]. The DE mode can propagate only in a certain range of directions, and therefore the surface magnon is seen in either Stokes or anti-Stokes side of the spectrum in ferromagnets [11]. We believe that $\text{Nd}_{0.5}\text{Ca}_{0.5}\text{MnO}_3$ is likely to possess magnetic domains expected in an orthorhombic system. This does not permit complete disappearance of the surface mode on one side of the spectrum at $H = 0$. However, application of a magnetic field aligns the domains and hence the asymmetry between Stokes and anti-Stokes intensities increases for the surface mode.

The higher surface magnon frequency relative to that of the bulk magnon implies that these are spin-wave excitations of a ferromagnet, for which frequencies are given by ($\omega_B = 2\pi\nu_B$) [12]

$$\omega_B^2 = \gamma^2(H + Dq^2)(H + Dq^2 + 4\pi M_S \sin^2 \theta), \quad (1)$$

where γ is the gyromagnetic ratio, H is the external applied magnetic field, D is the exchange constant, M_S is the saturation magnetisation and θ is the angle between q and M_S . The temperature dependence of ω_B is determined by M_S , as indeed seen in fig. 2(a). The Damon-Eshbach [9, 10] surface spin wave has frequency ($\omega_S = 2\pi\nu_S$)

$$\omega_S = \frac{\gamma}{2} \left[\frac{H}{\sin \theta'} + (H + 4\pi M_S) \sin \theta' \right] + \gamma D' q_{\parallel}^2, \quad (2)$$

where $D' \sim 2D$ [11] and θ' is the angle between q_{\parallel} and M_S . It can be seen that $\omega_S > \omega_B$ for magnons in a ferromagnet. This is, however, not the case for magnons in antiferromagnets [12].

For $H = 0$

$$2\pi\nu_S = \gamma(2\pi M_S \sin \theta') + \gamma D' q_{\parallel}^2. \quad (3)$$

The solid line in fig. 4(a) shows the fit of ν_S to eq. (3), giving $M_S \sin \theta' = 0.325$ T and $D' = 1.68$ eV \AA^2 . This gives a rough estimate of $D \sim 0.84$ eV \AA^2 , which is higher than the value measured by inelastic neutron scattering in the ferromagnetic phase of these manganites [13]. We should keep in mind that the S-mode is very weak and the range of q_{\parallel} is limited, which makes the accurate determination of D and M_S difficult. A large value of $4\pi M_S$ also implies that the changes in frequency of the bulk and surface magnons due to the applied field up to 0.3 T will be very small, in agreement with our experiments.

We now discuss the temperature variation of the scattered light intensity from spin waves via fluctuations in the dielectric constant ϵ arising due to spin-orbit coupling to the spin fluctuations. The scattered intensity is [9]

$$I(\omega) \propto \frac{\gamma M_S}{\omega} k_B T |GM_S \pm K|^2, \quad (4)$$

where G and K are magneto-optic constants coupling $\Delta\epsilon$ to transverse component of the magnetisation M_t and M_S : $\Delta\epsilon = KM_t + GM_S M_t$. The \pm signs refer to Stokes and anti-Stokes intensities. It can be seen that $I(\omega)$ will also follow the temperature dependence of saturation magnetisation, as seen in fig. 3(a).

The linewidth Γ of the Brillouin line associated with spin-waves arises from lifetime effects ($= 2/T_2$ for the transverse coupling, where $1/T_2$ is the spin-spin relaxation rate [14]) as well as from inhomogeneous broadening. This broadening is somewhat similar to that seen in electron spin-resonance [15]. The enhancement of Γ seen at T_{CO} can be due to critical magnetic fluctuations. The temperature dependence of the linewidth of the spectral function for the spin auto-correlation function due to critical fluctuations is given by $\Gamma(q) = \Gamma_0(q) f(1/q\xi)$, where $\Gamma_0(q)$ is the linewidth at T_C and $f(x)$ is a homogeneous complicated function of x [16]. Here ξ is the correlation length which diverges as $\xi \sim (T - T_C)^{-\nu}$, with $\nu \sim 0.6$. The function $f(x)$ is non-monotonic, it decreases as x decreases till $1/q\xi \sim 1$, but for lower values of $1/q\xi$ (*i.e.* $T \rightarrow T_C$) it increases. The enhancement of the Brillouin linewidth as T decreases from 300 to 250 K (see fig. 3(b)) corresponds to the increase in the function $f(1/q\xi)$ below $(q\xi)^{-1} < 1$.

A few words on why we do not see magnons due to the AFM state would be appropriate. The zero wave vector bulk magnon in antiferromagnet has frequency $\omega_B = \gamma(2B_E B_A + B_A^2)^{1/2}$, where B_E is the exchange field and B_A is the anisotropy field [12]. Usually $B_E \gg B_A$ and therefore $\omega_B \sim \gamma\sqrt{2B_E B_A}$. These frequencies are much higher than those in ferromagnet; *e.g.* $\omega_B \sim 8.7$ cm^{-1} in MnF_2 ($T_N \sim 100$ K) and $\omega_B \sim 52$ cm^{-1} in FeF_2 . The scattering cross-section is proportional to $\sqrt{B_A}$, and therefore the antiferromagnet tends to be a much poorer light scatterer [12].

Our results clearly demonstrate that magnetic excitations associated with ferromagnets are present at all temperatures, even below T_N . This is somewhat surprising and can be understood on the basis of the following considerations. The large peak in χ at T_{CO} is attributed to

FM correlations due to Zener double-exchange mechanism [13,17]. This is because below T_{CO} , the e_g electrons become self-trapped due to JT polarons. The resulting ordering of e_g orbitals allows strong superexchange interactions which gives rise to antiferromagnetism. However, above T_{CO} , the carriers are relatively free to move and the superexchange mechanism will be weak and locally undetermined. This allows Zener double exchange to operate. Another reason to see ferromagnetic magnons above T_{CO} could be the light scattering mechanism [14]. It is known that the transverse scattering cross-sections are usually much higher than the longitudinal ones below T_C corresponding to para-to-ferro transition as a result of non-zero spontaneous magnetisation. Above T_C , both the cross-sections are equal. The interesting aspect of light scattering from magnetic excitations is that the transverse scattering cross-section above T_C (*i.e.* in para state) is non-zero. For example, in FM CrBr₃, the intensity ratio $I(T)/I(T_C)$ is as high as ~ 0.6 for $T/T_C \sim 1.25$ [14]. This explains why we can observe spin-wave excitations in the Brillouin spectra in the PM phase above T_{CO} .

With regard to the presence of ferromagnetic magnons below T_{CO} , the recent report of a spin wave branch in neutron scattering experiments below T_N in La_{1-x}Ca_xMnO₃ ($x = 0.05$ and 0.08) is relevant [18]. This low-energy branch, fitted to $\omega = \omega_0 + Dq^2$, is attributed to magnetic excitations of a droplet with ferromagnetic correlation length of ~ 10 Å. Surprisingly, these spin excitations are well defined and have a propagating character even at small q , *i.e.* over distances larger than the droplet size. The presence of ferromagnetic excitations along with those of the AFM state have been related to the separation of the sample into two magnetic regions, induced by an electronic phase segregation. Our present results also support such a scenario in charge-ordered Nd_{0.5}Ca_{0.5}MnO₃. The increase in the susceptibility below 100 K (see fig. 2(b)) as well as seen in fig. 2(a) can be understood either as a mixture of ferromagnetic domains in AFM background or as a canted AFM state [13].

In summary, bulk and surface magnetic excitations have been seen in the Brillouin scattering of Nd_{0.5}Ca_{0.5}MnO₃. These excitations are associated with ferromagnetic correlations over the temperature range of 300 to 27 K. The presence of ferromagnetic droplets below T_{CO} suggests an electronic phase segregation, similar to the one proposed in other manganites. It would be of interest to carry out inelastic neutron scattering experiments on charge-ordered systems to look for ferromagnetic propagating modes below T_{CO} .

REFERENCES

- [1] RAO C. N. R. and RAVEAU B. (Editors), *Colossal Magnetoresistance, Charge-ordering and Related Properties of Manganese Oxides* (World Scientific, Singapore) 1998.
- [2] WOODWARD P. M., VOGT T., COX D. E., ARULRAJ A., RAO C. N. R., KAREN P. and CHEETHAM A. K., *Chem. Mater.*, **10** (1998) 3652.
- [3] ZENER C., *Phys. Rev.*, **82** (1951) 403; ANDERSON P. W. and HASEGAWA, *Phys. Rev.*, **100** (1955) 675.
- [4] MILLIS A. J., LITTLEWOOD P. B. and SHRAIMAN B. I., *Phys. Rev. Lett.*, **74** (1995) 5144.
- [5] VERMA C. M., *Phys. Rev. B*, **54** (1996) 7328.
- [6] MORI S., CHEN C. H. and CHEONG S.-W., *Phys. Rev. Lett.*, **81** (1998) 3972.
- [7] MORI S., KATSUFUJI T., YAMAMOTO N., CHEN C. H. and CHEONG S.-W., *Phys. Rev. B*, **59** (1999) 13573.
- [8] VOGT T., CHEETHAM A. K., MAHENDIRAN R., RAYCHAUDHURI A. K., MAHESH R. and RAO C. N. R., *Phys. Rev. B*, **54** (1996) 15303.
- [9] SANDERCOCK J. R., in *Light Scattering in Solids*, edited by M. CARDONA and GUNTHERÖDT G., Vol. **III** (Springer Verlag, Berlin) 1982, p. 173.
- [10] DAMON R. W. and ESHBACH J. R., *J. Phys. Chem. Solids*, **19** (1961) 308.

- [11] SANDERCOCK J. R. and WETTING W., *J. Appl. Phys.*, **50** (1979) 7784.
- [12] COTTAM M. G. and LOCKWOOD D. J., *Light Scattering in Magnetic Solids* (John Wiley, New York) 1986.
- [13] COX D. E., RADAELLI P. G., MAREZIO M. and CHEONG S.-W., *Phys. Rev. B*, **57** (1998) 3305.
- [14] HAYES W. and LOUDON R., *Scattering of Light by Crystals* (John Wiley, New York) 1978, p. 239.
- [15] GUPTA R., JOSHI J. P., BHAT S. V., SOOD A. K. and RAO C. N. R., *J. Phys. Condens. Matter*, **12** (2000) 6919.
- [16] RESIBOIS P. and PIETTE C., *Phys. Rev. Lett.*, **24** (1970) 514.
- [17] POLLERT E., KRUPICKA S. and KUZMICOVA E., *J. Phys. Chem. Solids*, **43** (1982) 1137.
- [18] HENNION M., MOUSSA F., BIOTTEAU G., RODRIGUEZ-CARVAJAL J., PINSARD L. and REVCOLEVSKI A., *Phys. Rev. Lett.*, **81** (1998) 1957; MOUSSA F., HENNION M., BIOTTEAU G., RODRIGUEZ-CARVAJAL J., PINSARD L. and REVCOLEVSKI A., *Phys. Rev. B*, **60** (1999) 12299.